Journal of *Marine Science and Engineering*

MDPI

Article

Development of Hydroacoustic Localization Algorithms for AUV Based on the Error-Corrected WMChan-Taylor Algorithm

Huibao Yang [1], Xiujing Gao [2,3], Bangshuai Li [4], Bo Xiao [4] and Hongwu Huang [1,2,3,4,*]

[1] School of Aerospace Engineering, Xiamen University, Xiamen 361000, China; yanghuibao@stu.xmu.edu.cn
[2] School of Smart Marine Science and Engineering, Fujian University of Technology, Fuzhou 350118, China
[3] Fujian Provincial Key Laboratory of Marine Smart Equipmeng, Fuzhou 350118, China
[4] State Key Laboratory of Advanced Design and Manufacturing Technology for Vehicle, Hunan University, Changsha 410008, China
* Correspondence: huanghongwu@fjut.edu.cn

Abstract: Autonomous underwater vehicles (AUVs) are susceptible to non-line-of-sight (NLOS) errors and noise bias at receiving stations during the application of hydroacoustic localization systems, leading to a degradation in positioning accuracy. To address this problem, this paper optimizes the Chan-Taylor algorithm. Initially, we propose the Weighted Modified Chan-Taylor (WMChan-Talor) algorithm, which introduces dynamic weights into the Chan algorithm to correct noise variance at measurement stations, thereby improving the accuracy of AUV positioning. Computer simulations validate the effectiveness of the WMChan-Taylor algorithm in enhancing positioning accuracy. To further address the accuracy degradation caused by noise deviations across different receiving stations, we introduce an error-corrected WMChan-Taylor algorithm. This algorithm utilizes a standard residual function to eliminate significant delays caused by large errors at receiving stations and applies standard residual weighting to improve the combined positioning solution. The performance of the error-corrected WMChan-Taylor algorithm is demonstrated through both computer and semi-physical simulation experiments, confirming its capability to isolate noisier stations and thus enhance overall positioning accuracy.

Keywords: autonomous underwater vehicle; hydroacoustic positioning systems; Chan-Taylor; weighted modified Chan-Taylor (WMChan-Taylor); error-corrected WMChan-Taylor

Citation: Yang, H.; Gao, X.; Li, B.; Xiao, B.; Huang, H. Development of Hydroacoustic Localization Algorithms for AUV Based on the Error-Corrected WMChan-Taylor Algorithm. *J. Mar. Sci. Eng.* **2024**, *12*, 974. https://doi.org/10.3390/jmse12060974

Academic Editor: Weicheng Cui

Received: 13 May 2024
Revised: 4 June 2024
Accepted: 6 June 2024
Published: 11 June 2024

1. Introduction

With the growing interest in oceanic exploration, autonomous underwater vehicles (AUVs) play a vital role in marine research activities, such as ocean pollution monitoring [1], marine biology exploration [2], and pipeline inspection [3]. To maximize the AUV's efficiency, reliable navigation information is essential, and precise positioning is mandatory for effective navigation and control [4]. AUVs employ a range of underwater positioning technologies, including underwater acoustic systems [5], inertial navigation systems [6], dead reckoning systems [7], and geophysical navigation systems [8]. Among these, underwater acoustic positioning systems are the most commonly used to localize AUVs. These systems calculate the AUV's position by analyzing acoustic propagation times using algorithms and refining the estimates. Key technologies include time of arrival (TOA) [9], time difference of arrival (TDOA) [10], angle of arrival (AOA) [11], and received signal strength indicator (RSSI) [12]. TDOA is particularly valued for its simplicity, real-time capabilities, and independence from time synchronization between the sound source and sensors, making it useful not only in underwater positioning but also in terrestrial wireless systems. Addressing the nonlinear optimization challenges of TDOA positioning typically involves three primary solution methods: linearization, nonlinear iterative, and hybrid localization algorithms [13–16].

Linear algorithms offer significant benefits, including straightforward computational processes, excellent real-time performance, and robust convergence. However, linearizing nonlinear positioning equations can degrade performance, particularly in noisy environments that significantly increase positioning errors [17]. Currently, existing TDOA methods typically require solving nonlinear hyperbolic equations, necessitating the use of a nonlinear iterative method. This process is computationally intensive and time-consuming. Kun et al. proposed an enhanced AUV-aided TDOA localization algorithm (EATLA) for underwater acoustic sensor networks (UASNs), which achieves relatively higher accuracy with smaller calculations and overcomes some traditional localization drawbacks [18]. To manage the high computational load from extensive observational data and potential local optima in the least squares method, Chen et al. applied the implicit function theorem to derive the Jacobian matrix for linear and circular measurement configurations [19]. This matrix serves as a constraint, and an optimization algorithm is used to enhance positioning accuracy in shallow water areas. Xu et al. proposed an iterative stepping algorithm that has been followed to solve the evaluation function and obtain the optimal positions of the sensors. The algorithm ensured that the computation complexity should remain limited, even when the number of sensors is increased [20]. To minimize errors, Lekkas et al. employed statistical testing to assess the quality distribution of observed values, thus improving positioning accuracy [21]. Furthermore, nonlinear iterative methods include Fang, SX, SI, and Taylor series expansions [22,23]. To reduce the location bias and improve location accuracy, Liang et al. presented a novel bias-reduced method based on an iterative constrained weighted least squares algorithm [24]. These methods; however, suffer from limitations such as inefficient use of measurement data and high initial precision requirements [25]. Furthermore, the success of these algorithms in achieving high-precision results presupposes that TDOA measurement errors are normally distributed. Nevertheless, the effectiveness of nonlinear iterative methods heavily relies on the accuracy of initial values. Imprecise initial values can cause the algorithm to diverge, failing to converge effectively to the true target value.

Hybrid localization algorithms combine various algorithms, such as least square and nonlinear expectation maximization (LS-NLEM) [26], semidefinite programming with weighted least squares (SDP-WLS) [27], and singular value decomposition with least squares (SVD-LS) [28], Chan-Taylor algorithm [29]. Research indicates that these algorithms offer superior accuracy under similar conditions and effectively mitigate slow convergence caused by inaccuracies in initial values. Moreover, they are less sensitive to external environmental changes compared to single-method approaches. However, underwater environments, characterized by their complexity and numerous obstructions, significantly impede the propagation of sound signals. Most signals received at stations are influenced by reflections and multipath effects, leading to significant non-line-of-sight (NLOS) errors. These non-Gaussian TDOA values compromise the efficacy of localization algorithms. Conventional methods like least squares, Chan's algorithm, and Taylor series expansion often overlook these NLOS effects. To address these challenges, researchers have developed wireless sensor network localization algorithms using particle swarm optimization (PSO) to reduce the biases typical of traditional methods [30–32]. Additionally, Chen et al. introduced an advanced TDOA/AOA localization method utilizing the dandelion optimization algorithm, which enhances optimization performance by integrating optimal solutions from two populations through a multi-objective mechanism [33]. Nevertheless, as TDOA and AOA errors increase, the accuracy of the final convergence results deteriorates. Furthermore, the current position solution process fails to account for noise deviations between different stations under NLOS conditions, adversely affecting localization accuracy.

To address the issues discussed, this paper introduces a novel position-solving algorithm for the hydroacoustic localization system of AUV. This novel algorithm estimates the noise variance within the Chan-Taylor framework to minimize NLOS errors and enhance positioning accuracy by defining a standard residual function that isolates receiving

stations with significant noise deviations. Initially, the weighted modified Chan-Taylor (WMChan-Taylor) was developed based on the Chan-Taylor algorithm. The WMChan-Taylor algorithm addresses the issue of diminished positioning accuracy, which arises from substantial initial errors in the Chan-Taylor algorithm due to NLOS conditions, by integrating a dynamic weighting mechanism. Subsequently, the WMChan-Taylor algorithm is optimized to mitigate the impact of noise bias at the receiving station. An error-corrected version of this algorithm is then proposed, which employs a standard residual function as an evaluative metric. This function helps eliminate receiving stations with high measurement noise variance and applies residual weighting to the position solution combinations for enhanced optimization and improved positioning accuracy.

The rest of this paper is organized as follows. Section 2 outlines the TDOA system model and the Chan-Taylor algorithm. Section 3 discusses the WMChan-Taylor algorithm and the error-corrected WMChan-Taylor algorithm introduced in this paper. The proposed algorithms are then simulated and analyzed in Section 4. Section 5 further validates these algorithms by establishing a semi-physical simulation platform. Finally, Section 6 concludes the paper and suggests potential avenues for future research.

2. System Model

This section presents the mathematical model of an acoustic localization system for AUVs that utilizes the TDOA system. It further analyzes the commonly used Chan-Taylor algorithm within this framework and identifies its limitations.

2.1. Time Difference of Arrival System

Hydroacoustic positioning technology utilizes a network of hydrophone buoys and seafloor stations to acoustically determine the positions of AUVs. In this system, the AUV is equipped with an interrogator that periodically transmits interrogation pulses. These pulses are received and processed by either a seafloor station or a buoy, which then sends a return acknowledgment signal to the interrogator. The system calculates the distance between the interrogator and the transponder by measuring the acoustic round-trip time and uses this data to determine the AUV's position relative to each transponder, thereby ensuring precise positioning. The fundamental measurement principle of this technology is based on the propagation time of the acoustic signal, which is mathematically represented as follows:

$$(x_i - x)^2 + (y_i - y)^2 + (z_i - z)^2 = c^2(t_i - t)^2 \tag{1}$$

In Equation (1), (x_i, y_i, z_i) represents the ith array element, c denotes the underwater speed of sound, and t_i indicates the moment when the signal is received by array element i, $i = 1, 2, \cdots, N$. (x, y, z) specifies the three-dimensional (3D) coordinates of the target point, and t corresponds to the moment of signal emission relative to the receiver's clock.

Hydroacoustic positioning techniques vary based on time synchronization conditions and can be classified into two categories: synchronous and non-synchronous systems. In non-synchronous systems, the sound source clock is not synchronized with the measurement clock, represented by $t \neq 0$. High-precision positioning requires the elimination of clock error interference, denoted by Δt. When the sound source and receiving system times are not synchronized, Equation (1) is adapted to a non-synchronous positioning model.

As depicted in Figure 1, once the target depth is established, measuring the TDOA between the source on the AUV and various base array elements enables the derivation of quadratic equations that define a hyperbolic curve [10]. Assuming that the coordinates of the AUV are represented by (x, y, z) and those of the receiver by (x_i, y_i, z_i). The distance r_i between the moving AUV and the receiver satisfies the following condition:

$$\begin{aligned} r_i^2 &= (x_i - x)^2 + (y_i - y)^2 + (z_i - z)^2 \\ &= K_i - 2x_i x - 2y_i y - 2z_i z + x^2 + y^2 + z^2 \end{aligned} \tag{2}$$

where $K_i = x_i^2 + y_i^2 + z_i^2$.

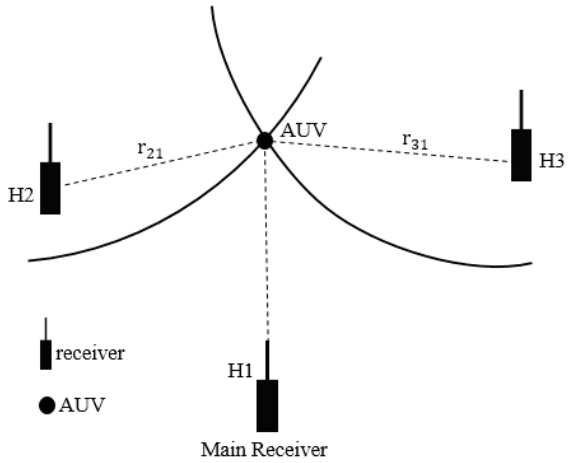

Figure 1. TDOA positioning model.

Assuming $r_{i,1}$ represents the difference between the distance from the AUV to the ith $(i > 1)$ receiver and the distance to the first receiver, it can be expressed as follows:

$$r_{i,1} = r_i - r_1 \tag{3}$$

where $r_{i,1} = cd_{i,1}$, $d_{i,1}$ is TDOA values.

From Equation (3), there is:

$$r_{i,1}^2 + 2r_{i,1}r_1 + r_1^2 = K_i - 2x_i x - 2y_i y - 2z_i z + x^2 + y^2 + z^2 \tag{4}$$

The matrix of Equation (3) is expressed as:

$$2(x_{i,1}, y_{i,1}, z_{i,1}, r_{i,1})(x, y, z, r_1)^T = K_i - K_1 - r_{i,1}^2 \tag{5}$$

where $x_{i,1} = x_i - x_1$, $y_{i,1} = y_i - y_1$, $z_{i,1} = z_i - z_1$.

When x, y and r are considered unknown variables, other parameters can be practically measured. Once the depth z of the AUV is determined through depth sensor measurements, and r is dependent on x and y, only x and y remain unknown. With three receivers configured, two linear equations can be established to derive a unique solution for x and y. The Chan-Taylor algorithm enhances accuracy when more than three receivers are utilized, and the number of equations surpasses the number of unknowns.

2.2. Chan-Taylor Algorithm

In TDOA positioning systems, the Taylor series expansion algorithm serves as both a common positional technique and a recursive method for solving nonlinear equations. Based on the Taylor median theorem, this algorithm expands the positional equation using a Taylor series, which theoretically includes infinitely many terms. In practice, only the first-order derivative term is retained to minimize computational complexity. Nevertheless, this algorithm's sensitivity to initial estimates can result in slow convergence if the starting estimate is poorly chosen. To address this issue, the Chan algorithm can be employed to initially determine the observed data's position, which then serves as the initial input for the Taylor series expansion algorithm.

The Chan algorithm provides an analytical solution to the hyperbolic intersection model system of equations, distinguished by its explicit analytical formulation and minimal computational demands. In the AUV motion process, it is assumed that the depth z is known and variable $z_a = \left[z_p^T, r_1\right]^T$ remains unknown. The error vector associated with TDOA noise is derived from Equation (5) as follows:

$$\boldsymbol{\Psi} = \boldsymbol{h} - \boldsymbol{G}_a \boldsymbol{z}_a^0 \tag{6}$$

where $\boldsymbol{h} = \frac{1}{2}\begin{bmatrix} K_1 - K_2 + r_{2,1}^2 \\ K_1 - K_3 + r_{3,1}^2 \\ \vdots \\ K_1 - K_N + r_{n,1}^2 \end{bmatrix}$, $\boldsymbol{G_a} = \begin{bmatrix} x_{2,1} & y_{2,1} & z_{2,1} & r_{2,1} \\ x_{3,1} & y_{3,1} & z_{3,1} & r_{3,1} \\ & & \vdots & \\ x_{n,1} & y_{n,1} & z_{n,1} & r_{n,1} \end{bmatrix}$.

Where the maximum likelihood estimation of $\boldsymbol{z_a}$ is

$$\boldsymbol{z_a} = \left(\boldsymbol{G_a}^T \boldsymbol{\varphi}^{-1} \boldsymbol{G_a}\right)^{-1} \boldsymbol{G_a}^T \boldsymbol{\varphi}^{-1} \boldsymbol{h} \tag{7}$$

where $\boldsymbol{\varphi}$ is the error matrix, $\boldsymbol{\varphi} = c^2 \boldsymbol{B} \boldsymbol{Q} \boldsymbol{B}^T$, c is the speed of sound, $\boldsymbol{Q}$ is the Gaussian error covariance matrix of the measurements. $B = diag(r_2^0, r_3^0, \cdots, r_n^0)$, r_n^0 is the actual distance from the nth receiver signal to the AUV.

The Chan algorithm treats x, y, r_1 as a distinct variable and assumes that the mean of $\boldsymbol{z_a}$ represents the actual value when the resultant TDOA measurement error is minimal.

Define $z_{a,1} = x^0 + e_1$, $z_{a,2} = y^0 + e_2$, $z_{a,3} = z^0 + e_3$, where e_1, e_2 and e_3 represent the estimation errors of $\boldsymbol{z_a}$. A system of equations is derived by subtracting the first two elements of $\boldsymbol{z_a}$ from x_1 and y_1, then squaring these elements.

$$\boldsymbol{\varphi'} = \begin{bmatrix} (z_{a,1} - x_1)^2 \\ (z_{a,2} - y_1)^2 \\ z_{a,3}^2 \end{bmatrix} - \begin{bmatrix} 1 & 0 \\ 0 & 1 \\ 1 & 1 \end{bmatrix} \begin{bmatrix} (x - x_1)^2 \\ (y - y_1)^2 \end{bmatrix} \tag{8}$$

The covariance matrix of $\boldsymbol{\varphi'}$ is $\boldsymbol{\phi'} = \left[\boldsymbol{\varphi'} \boldsymbol{\varphi'}^T\right] = 4\boldsymbol{B'} \mathrm{cov}(\boldsymbol{z_a}) \boldsymbol{B'}$, where $\boldsymbol{B'} = diag(x^0 - x_1, y^0 - y_1, r_1^0)$. Then, the maximum likelihood estimation of $\boldsymbol{z'_a}$ is:

$$\boldsymbol{z'_a} = \left(\boldsymbol{G'_a}^T \boldsymbol{\varphi'}^{-1} \boldsymbol{G'_a}\right)^{-1} \boldsymbol{G'_a}^T \boldsymbol{\varphi'}^{-1} \boldsymbol{h'} \tag{9}$$

Determine whether $\boldsymbol{z_p} = \sqrt{\boldsymbol{z'_a}} + \begin{bmatrix} x_1 \\ y_1 \end{bmatrix}$ or $\boldsymbol{z_p} = -\sqrt{\boldsymbol{z'_a}} + \begin{bmatrix} x_1 \\ y_1 \end{bmatrix}$ using Equation (9). This allows the identification of both the positive and negative values of $\sqrt{\boldsymbol{z'_a}}$, ultimately providing the initial coordinates (x_0, y_0).

A Taylor expansion at the initially guessed target location (x_0, y_0), which disregards components higher than the second order, is performed as follows.

$$\boldsymbol{\psi} = \boldsymbol{h_t} - \boldsymbol{G_t} \boldsymbol{\delta} \tag{10}$$

where $\boldsymbol{\delta} = \begin{bmatrix} \Delta x \\ \Delta y \end{bmatrix}$, $\boldsymbol{h_t} = \begin{bmatrix} r_{2,1} - (r_2 - r_1) \\ r_{3,1} - (r_3 - r_1) \end{bmatrix}$, $\boldsymbol{G_t} = \begin{bmatrix} \frac{x_1 - x_0}{r_1} - \frac{x_2 - x_0}{r_2} & \frac{y_1 - y_0}{r_1} - \frac{y_2 - y_0}{r_2} \\ \frac{x_1 - x_0}{r_1} - \frac{x_3 - x_0}{r_3} & \frac{y_1 - y_0}{r_1} - \frac{y_3 - y_0}{r_3} \end{bmatrix}$.

Where $\boldsymbol{\psi}$ is the measurement error vector and $r_i (i = 1, 2, \cdots, n)$ is the distance between the initial position and each receiving station. The weighted least squares solution of Equation (10) is:

$$\boldsymbol{\delta} = \left(\boldsymbol{G_t}^T \boldsymbol{Q}^{-1} \boldsymbol{G_t}\right)^{-1} \boldsymbol{G_t}^T \boldsymbol{Q}^{-1} \boldsymbol{h_t} \tag{11}$$

$\boldsymbol{Q}$ represents the covariance matrix of the delay difference measurements, it is defined as follows:

$$\begin{aligned} x'_0 &= x_0 + \Delta x \\ y'_0 &= y_0 + \Delta y \end{aligned} \tag{12}$$

Repeat the process until Δx and Δy sufficiently small to meet the predefined limit ξ.

$$|\Delta x| + |\Delta y| < \xi \tag{13}$$

The (x'_0, y'_0) obtained at this stage represents the position estimation of the target.

The main steps of the Chan-Taylor algorithm are illustrated in Figure 2, with the processes described as follows [29].

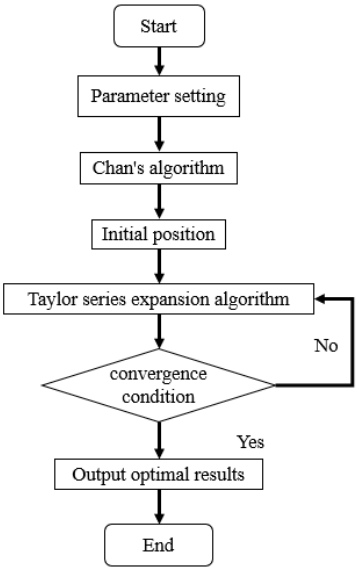

Figure 2. Flowchart of the Chan-Taylor algorithm.

Step 1. Set parameters such as the number of iterations, convergence threshold, and other critical parameters.

Step 2. Use the Chan algorithm for initial target position.

Step 3. Implement iterative optimization using the Taylor series expansion algorithm. Begin with the initial position from step 2 and iteratively refine this estimate to approach the true position.

Step 4. After each iteration, verify whether the preset convergence conditions are met.

3. Optimized Localization Algorithms

3.1. Weighted Modified Chan-Taylor Algorithm

The Chan-Taylor algorithm employs the Chan algorithm to address the recursive computation of initial values required by the Taylor series expansion algorithm. The precision of the initial values obtained significantly influences the outcomes and convergence speed of the Taylor series expansion. Typically, the Chan algorithm necessitates the estimation of the measurement noise matrix $\boldsymbol{Q}$, during the solution process. $\boldsymbol{Q}$ is variable in practice, and its fluctuations affect the accuracy of the Chan algorithm. Consequently, to enhance the initial value determination in scenarios with NLOS errors, the weighted modified Chan-Taylor (WMChan-Taylor) algorithm has been developed.

The AUV obtains depth z from a depth sensor. Assuming that M (M > 3) receiving stations are involved in localization, the system of equations formed by any two of the M-1 equations from Equation (6) yields a unique solution. The solutions for the various systems of equations are determined separately for each (x_k, y_k) $(k = 1, 2, \cdots, n)$, and a residual function is subsequently constructed as follows:

$$e_i(x_k, y_k) = r_{i1} - r_{ik} \tag{14}$$

Since z is known, it follows that $r_{i1} = \sqrt{(x_i - x)^2 + (y_i - y)^2} - \sqrt{(x_1 - x)^2 + (y_1 - y)^2}$, $r_{ik} = \sqrt{(x_i - x_k)^2 + (y_i - y_k)^2} - \sqrt{(x_1 - x_k)^2 + (y_1 - y_k)^2}$.

According to Equation (14), the residuals e_i from each equation are calculated, and the residual $e_{\min}$ with the smallest absolute value is identified to construct the $\boldsymbol{Q}$ matrix.

$$\boldsymbol{Q} = diag[e_{\min}, e_{\min}, \cdots, e_{\min}] \tag{15}$$

Flowchart of the WMChan-Taylor is shown in Figure 3, with its main steps as flows.

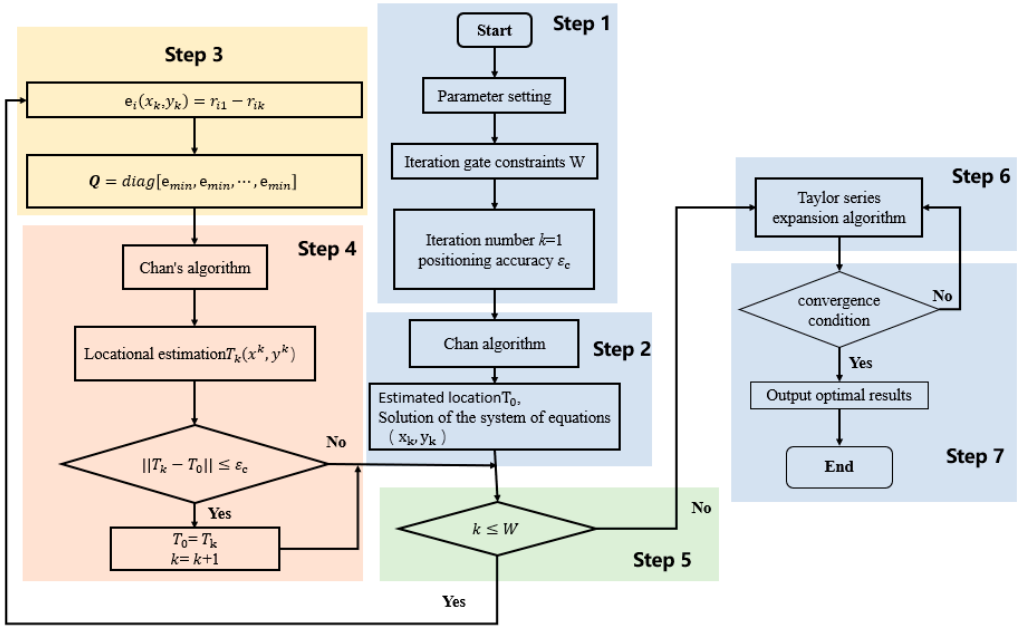

Figure 3. Flowchart of the WMChan-Taylor algorithm.

Step 1. Set the parameters, including the number of iterations, iteration threshold, positioning accuracy, number of stations, initial measurement noise matrix, and other relevant parameters.

Step 2. Use the Chan algorithm for positioning to determine the estimated position $T_0(x, y)$ and solve the system equations, obtaining solution (x_k, y_k).

Step 3. Calculate the residual $e_i(x_k, y_k) = r_{i1} - r_{ik}$ and construct a new measurement noise matrix $\boldsymbol{Q} = diag[e_{\min}, e_{\min}, \cdots, e_{\min}]$.

Step 4. Iterate the Chan algorithm for weight estimation. Calculate $T_k(x^k, y^k)$ based on the newly constructed measurement noise matrix $\boldsymbol{Q}$, verify the accuracy with $T_0(x, y)$, and update $T_0(x, y)$ and k.

Step 5. At the end of each iteration, assess whether the number of iterations k is less than W. If this condition is met, proceed to step 4. Otherwise, use the results as input for the Taylor series expansion algorithm.

Step 6. Implement the Taylor series expansion algorithm by taking the results of step 5 as the new initial value, and iterate the algorithm accordingly.

Step 7. If the algorithm satisfies the predefined convergence condition, terminate the iterations and output the final global optimal solution. If it does not meet the convergence condition, establish the current iteration result as the new initial value for the next round of the Taylor series expansion algorithm and continue the iterations.

3.2. Error-Corrected WMChan-Taylor Algorithm

The WMChan-Taylor algorithm enhances the accuracy of the Chan-Taylor algorithm in scenarios with NLOS errors by adjusting the measurement noise matrix Q of the Chan algorithm. However, the transmitted positioning signals may be obstructed by obstacles during AUV operations, and variations in noise across different receiving stations can lead to significant discrepancies in delay estimation results. Consequently, results from stations with substantial errors require correction. To address this problem, a standard residual function is established to exclude position estimates with significant errors, thereby optimizing the combination of delay estimation solutions. Subsequently, the aggregated position solutions are further refined by applying standard residual weighting to the positioning errors of the algorithm.

The standard residual function was calculated using the following formula:

$$C_c(x_0, y_0, \boldsymbol{T}_j) = \frac{\left[\sum_{i \in j} |r_{i1} - d_{i0}|\right]}{size(\boldsymbol{T}_j)} \tag{16}$$

where $\boldsymbol{T}_j$ represents the set of solved matrices for the stations, $\boldsymbol{T}_j$ is the first station serving as the reference, and the remaining stations form the j combinations. $d_{i0} = \sqrt{(x_i - x_0)^2 + (y_i - y_0)^2} - \sqrt{(x_1 - x_0)^2 + (y_1 - y_0)^2}$.

The formula used to calculate the position based on standard residual weighting is as following.

$$T = \frac{\left(\sum\limits_{\mathrm{j}=1}^{n} [x_0, y_0] {C_c}^{-1}(x_0, y_0, \boldsymbol{T}_j)\right)}{\sum\limits_{j=1}^{n} {C_c}^{-1}(x_0, y_0, \boldsymbol{T}_j)} \tag{17}$$

A flowchart of the error-corrected WMChan-Taylor algorithm is depicted in Figure 4, with the main steps outlined as follows:

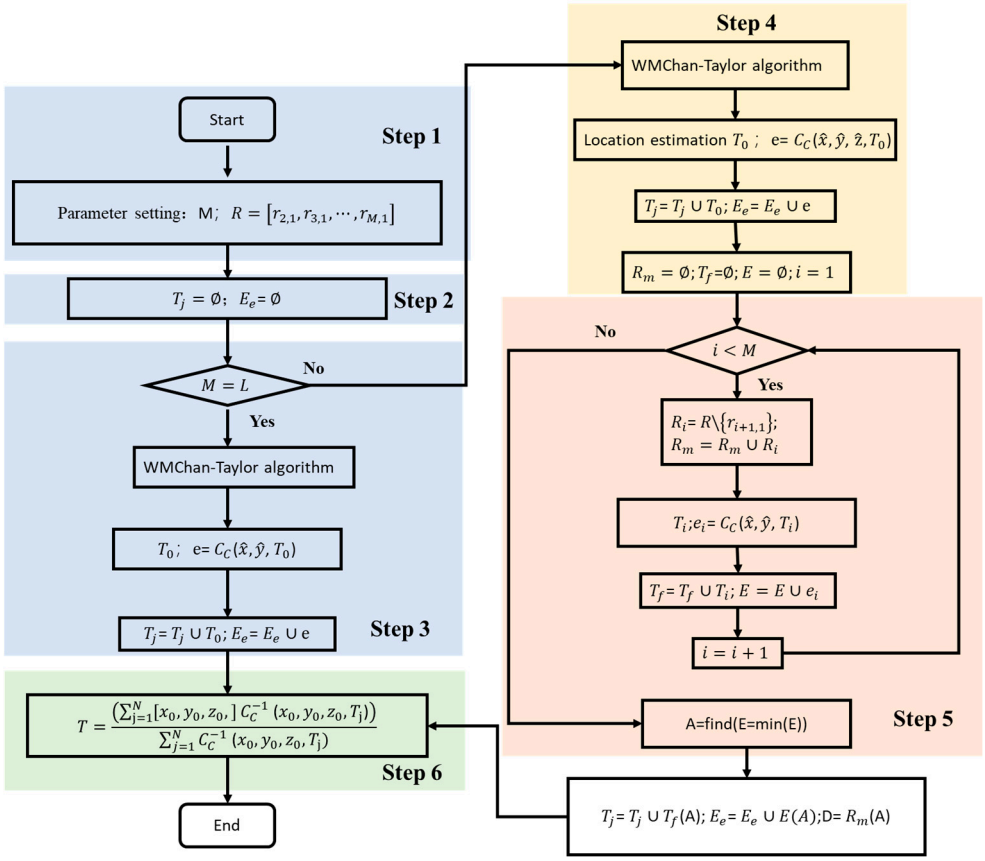

Figure 4. Flowchart of the error-corrected WMChan-Taylor algorithm.

Step 1. Set parameters, including the determination of the number of stations and convergence conditions.

Step 2. Determine the minimum number of stations L required in the location-solving process and select the appropriate scheme.

Step 3. If L represents the minimum number of stations, the WMChan-Taylor algorithm is executed to determine the position fixing results and calculate the standard residuals.

Step 4. When M exceeds L, the WMChan-Taylor algorithm is implemented, utilizing delay estimation data from all stations to determine positional location fixing results and

standard residuals. These results are stored in the target candidate set $\boldsymbol{T}_j$ and the standard residual selection set E_e.

Step 5. Use the station as a reference and sequentially extract the ith time delay value to form a combination of time delay values. Then, solve for the position based on this combination and calculate the target position along with the corresponding residuals.

Step 6. Retain the smallest standard residual in step 5 and compute the weighted position using Equation (17).

4. Analysis of the Simulation Results

During the simulation, the AUV's simulated motion trajectory consists of four linear segments and three semicircular segments, as shown in Figure 5. This type of trajectory is commonly used by AUVs for searching and exploration. Since the AUV's depth does not significantly change over short periods of time during missions and the depth sensor can provide highly accurate data in practical applications, the AUV simulates planar motion at a constant depth.

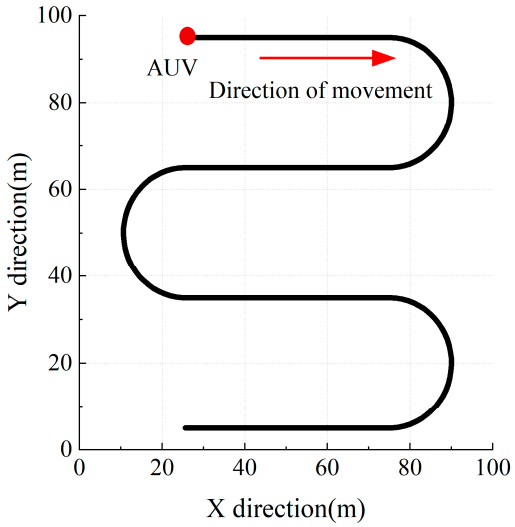

Figure 5. The AUV's motion trajectory.

In the simulation setup, the number of receiving stations is four, with coordinates H1 (0, 0), H2 (0, 200), H3 (200, 200), and H4 (0, 200). H1 serves as the central station. The position of each station is measured in meters. The AUV starts at an initial position of (25, 95) with a depth of 3 m underwater. Since the AUV's depth is fixed, the speed of sound is set to 1540 m/s, and the number of sampling points is 496. The Bellhop ray model is utilized to construct the hydroacoustic channel model. The key parameters in the environmental modeling process using Bellhop are set as follows. Assuming a water depth of 5000 m, a flat seafloor type, a seafloor sound velocity of 1500 m/s, a seafloor density of 1.8 g/cm^3, and a seafloor attenuation coefficient of 0.8 dB·λ^{-1}. The Munk deep-sea acoustic velocity profiles, with boundaries between depths of 0 and 5000 m, are selected for the acoustic field simulation. During positioning, the transducer positioning error is 10 cm, and the ranging error due to time delay is 5 cm.

4.1. Simulation Analysis of WMChan-Taylor Algorithm

In the simulation process, the value of ξ_c in the WMChan-Taylor algorithm is set to 0.01, and the iteration threshold W is set to 100. To compare the positioning effects of different algorithms under varying measurement noise variances, the position error

Formula (22) and the root mean square error (RMSE) [34] formula are used to evaluate the accuracy of the proposed algorithm.

$$RMS = \sqrt{(\overline{x}_i - x_i)^2 + (\overline{y}_i - y_i)^2} \tag{18}$$

In the formula, $\overline{x}_i$ and $\overline{y}_i$ represent the estimated values in the X and Y directions at the ith moment, respectively. x_i and y_i denote the actual values in the X and Y directions at the same moment. The larger the RMS value, the greater the error of the algorithm and the lower its accuracy. Conversely, the smaller the RMS value, the higher the positioning accuracy of the algorithm.

The positioning results of the Chan, Chan-Taylor, and WMChan-Taylor algorithms are shown in Figures 6 and 7 when the measurement noise variance σ is set to 0.1 ms. As illustrated in Figure 6, the positioning results of all three algorithms remain relatively stable. Figure 7 shows that the maximum RMS value of the Chan algorithm is 0.339 m, while the maximum RMS values of the Chan-Taylor and WMChan-Taylor algorithms are 0.313 m and 0.312 m, respectively. This indicates that the Chan-Taylor algorithm and the WMChan-Taylor algorithm optimize the positioning result of the Chan algorithm.

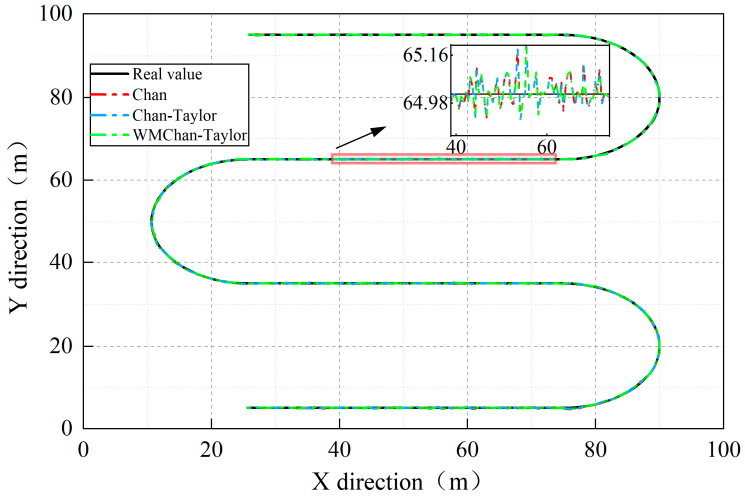

Figure 6. The localization results of the Chan, Chan-Taylor, and WMChan-Taylor algorithms (σ = 0.1 ms).

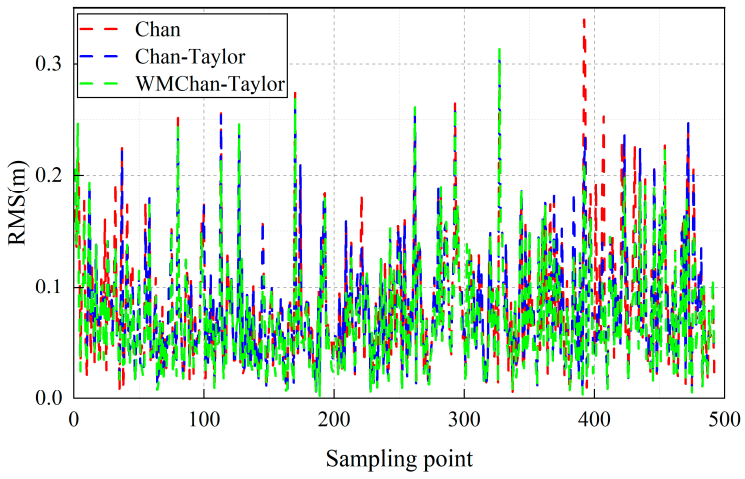

Figure 7. Variations in the RMS values of the Chan, Chan-Taylor, and WMChan-Taylor algorithms (σ = 0.1 ms).

As shown in Table 1, the changes in the RMS error values for both the Chan-Taylor and WMChan-Taylor algorithms are not significant, primarily because the initial error values in the Chan algorithm are small. The RMSE values of the WMChan-Taylor algorithm in the X and Y directions are 0.0602 m and 0.0677 m, respectively, while those of the Chan-Taylor algorithm are 0.0652 m and 0.0721 m. This indicates that the WMChan-Taylor algorithm is more stable than the Chan-Taylor algorithm in terms of computational results when σ = 0.1 ms.

Table 1. Comparison of the positioning parameters in the Chan, Chan-Taylor, and WMChan-Taylor algorithms (σ = 0.1 ms).

Algorithm	RMS (m)		RMSE (m)	
	maximum value	average value	X direction	Y direction
Chan	0.339	0.083	0.0663	0.0762
Chan-Taylor	0.313	0.081	0.0652	0.0721
WMChan-Taylor	0.312	0.078	0.0602	0.0677

When the measurement noise variance σ is set to 0.5 ms, the localization results of the Chan, Chan-Taylor, and WMChan-Taylor algorithms are shown in Figures 8 and 9. As the measurement noise variance increases, the localization error of the Chan algorithm begins to rise relative to previous results. As shown in Figure 9, the RMS value of the Chan algorithm changes significantly, reaching a maximum value of 3.241 m. Since the Chan-Taylor and WMChan-Taylor algorithms both use the Chan algorithm's results as the initial value for positioning, the localization error of the Chan algorithm increases as its results increase. Therefore, as the localization error of the Chan algorithm increases, the RMS values of these two algorithms also increase, reaching a maximum value of 1.437 m for both the Chan-Taylor and WMChan-Taylor algorithms. This indicates that both algorithms limit the propagation of errors in the Chan algorithm.

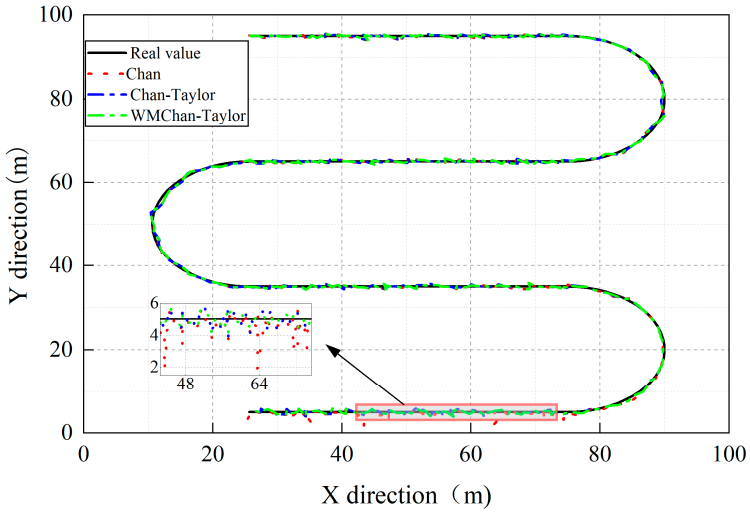

Figure 8. The localization results of the Chan, Chan-Taylor, and WMChan-Taylor algorithms (σ = 0.5 ms).

In comparing the average RMS values, the Chan-Taylor algorithm reduces the average error of the Chan algorithm by 0.056 m. Meanwhile, the WMChan-Taylor algorithm reduces the average error of the Chan algorithm by 0.083 m, outperforming the Chan-Taylor algorithm, as shown in Table 2. Regarding the RMSE values in the X and Y directions, the WMChan-Taylor algorithm achieves smaller errors, with 0.2985 m in the X direction and 0.3221 m in the Y direction, compared to 0.3319 m in the X direction and 0.3519 m in the Y direction for the Chan-Taylor algorithm. This demonstrates that the WMChan-Taylor

algorithm improves the overall system's localization stability through threshold values and iterative optimization.

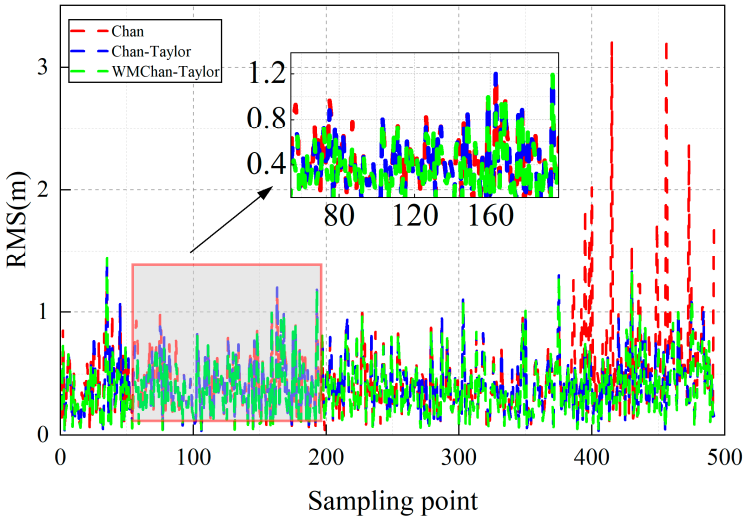

Figure 9. Variations in the RMS values of the Chan, Chan-Taylor, and WMChan-Taylor algorithms ($\sigma = 0.5$ ms).

Table 2. Comparison of the positioning parameters in the Chan, Chan-Taylor, and WMChan-Taylor algorithms ($\sigma = 0.5$ ms).

Algorithm	RMS (m)		RMSE (m)	
	maximum value	average value	X direction	Y direction
Chan	3.241	0.471	0.4782	0.3427
Chan-Taylor	1.437	0.415	0.3319	0.3519
WMChan-Taylor	1.437	0.358	0.2985	0.3221

Further comparisons of the localization results from the Chan, Chan-Taylor, and WMChan-Taylor algorithms reveal simulation outcomes in Figures 10 and 11. These simulations used a measurement noise variance of 1 ms as an illustrative example. As the measurement noise variance increases, the localization error of the Chan algorithm becomes more noticeable. Since both the Chan-Taylor and WMChan-Taylor algorithms use the results of the Chan algorithm as the initial value, when the error reaches a maximum value of 4.532 m, the WMChan-Taylor algorithm applies a weighting correction by estimating the measurement noise. Although the effect of this correction is not significant, the maximum error of the WMChan-Taylor algorithm is 2.841 m, compared to 2.871 m for the Chan-Taylor algorithm. As shown in Table 3, the average error of the WMChan-Taylor algorithm is 0.781 m, which is lower than the 0.813 m mean error of the Chan-Taylor algorithm. The difference between the two is 0.032 m, representing a decrease in effectiveness compared to the results under the conditions shown in Table 2.

Table 3. Comparison of the positioning parameters in the Chan, Chan-Taylor, and WMChan-Taylor algorithms ($\sigma = 1$ ms).

Algorithm	RMS (m)		RMSE (m)	
	maximum value	average value	X direction	Y direction
Chan	4.532	0.985	0.7486	0.9274
Chan-Taylor	2.871	0.813	0.6606	0.6936
WMChan-Taylor	2.841	0.781	0.5930	0.6637

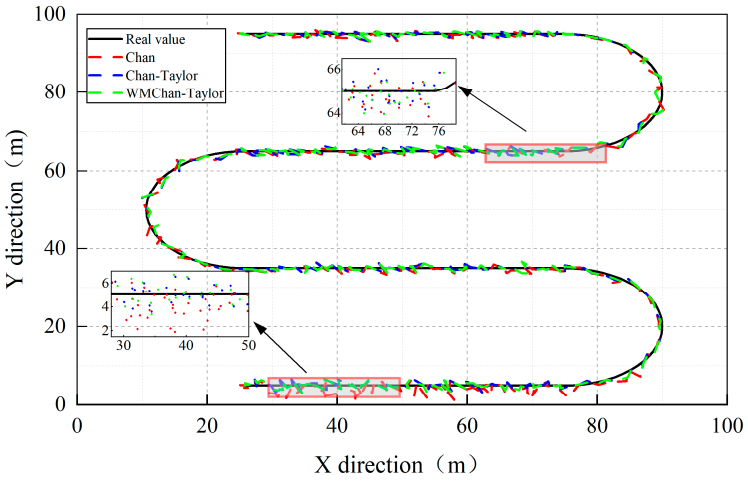

Figure 10. The localization results of the Chan, Chan-Taylor, and WMChan-Taylor algorithms (σ = 1 ms).

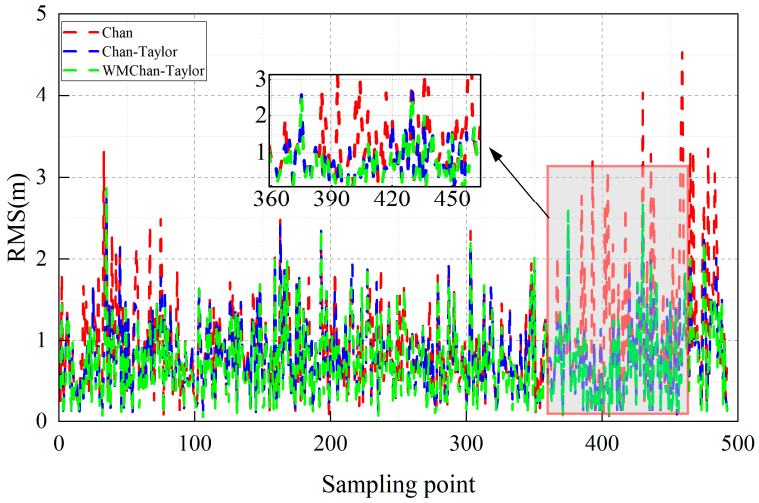

Figure 11. Variations in the RMS values of the Chan, Chan-Taylor, and WMChan-Taylor algorithms (σ = 1 ms).

The above analyses indicate that the errors of the Chan, Chan-Taylor, and WMChan-Taylor algorithms all increase with the rise in measurement error. Among them, the localization accuracy of the Chan algorithm decreases significantly. By employing the Chan-Taylor and WMChan-Taylor algorithms, localization accuracy can be improved to a certain extent. The WMChan-Taylor algorithm has better stability and localization accuracy than the Chan-Taylor algorithm by iteratively optimizing the localization results through measurement noise estimation.

4.2. Simulation Analysis of Error-Corrected WMChan-Taylor Algorithm

To analyze the effect of the error-corrected WMChan-Taylor algorithm, the total number of receiving stations M is set to 4 during the simulation, considering only motion in the horizontal plane. Consequently, the minimum number of stations L required for positional solutions is 3. All other parameters are identical to those used in the WMChan-Taylor algorithm.

From the analysis results in Section 4.1, it can be observed that when the noise variance σ is 1 ms, the WMChan-Taylor algorithm exhibits significant localization error. Therefore, the effect of the error-corrected WMChan-Taylor algorithm can be verified by varying the noise variance. To compare the impact of changes in noise variance on localization results

across different receiving stations, Figure 12 illustrates the process of measuring noise variance changes at receiving stations 3 and 4.

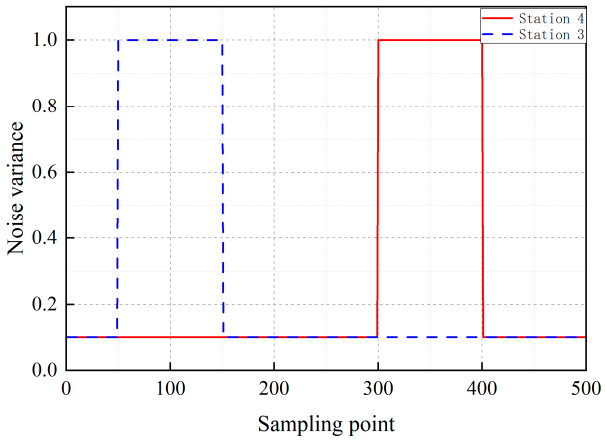

Figure 12. Changes in the noise variance at the receiving station.

During the simulation, the measurement noise error of receiving station 3 changes from the 50th sampling point to the 150th sampling point, while the measurement noise error of the receiving station 4 changes from σ = 0.1 ms to σ = 1 ms between the 300th and 400th sampling points. At other times, the measurement noise error of the receiving stations remains constant. All other simulation conditions are consistent with those in Section 4.1.

The simulation results of the noise variance of the receiving stations under NLOS conditions are shown in Figures 13 and 14. When the measured noise variance changes, the WMChan-Taylor algorithm does not correct the receiving stations that exhibit high measurement variance. As illustrated in Figure 13, excessive measurement noise variance cannot be mitigated through weight correction, leading to significant deviations in the localization results. Consequently, the 50th to 150th and the 300th to 400th sampling points show an increase in the RMS value of the localization error. The WMChan-Taylor algorithm produces the largest RMS deviation from the 50th to the 150th sampling point, with a maximum deviation of 2.683 m, and from the 300th to the 400th sampling point, with a maximum deviation of 3.340 m.

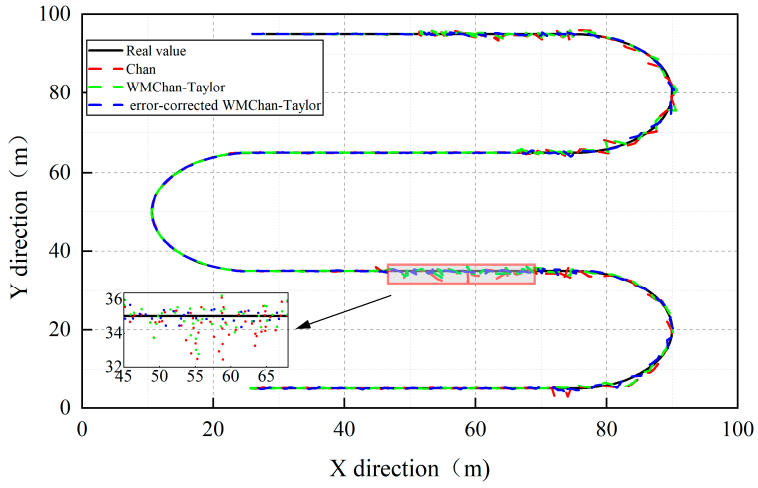

Figure 13. The localization results of the error-corrected WMChan-Taylor and WMChan-Taylor algorithms.

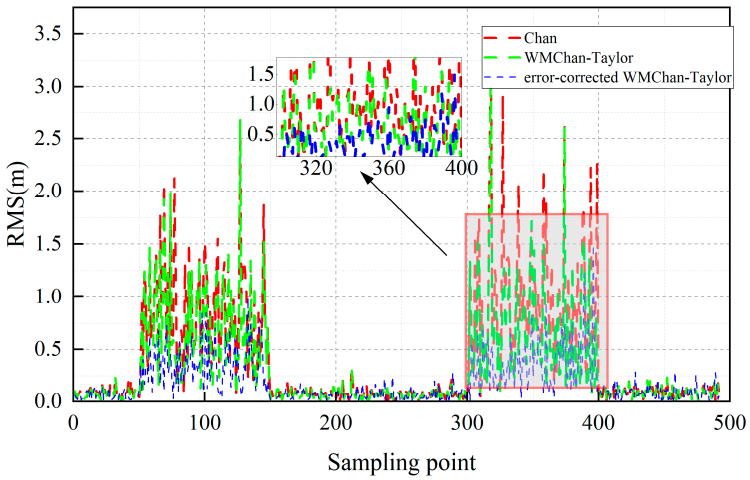

Figure 14. Variations in the RMS values of the error-corrected WMChan-Taylor and WMChan-Taylor algorithms.

Compared to the WMChan-Taylor algorithm, the error-corrected WMChan-Taylor algorithm calculates the target location and corresponding residuals by combining different station solution equations and applying a weighting function for weighted correction. This approach reduces the impact of receiving stations with high measurement noise variance on the localization results. The maximum RMS deviation ranges from 0.993 m between the 50th and 150th sampling points to 1.496 m between the 300th and 400th sampling points. These values are smaller than those of the WMChan-Taylor algorithm, indicating improved localization accuracy.

The RMSE values of the error-corrected WMChan-Taylor and WMChan-Taylor algorithms are presented in Table 4. The RMSE values in the X and Y directions for the error-corrected WMChan-Taylor algorithm are 0.1729 m and 0.2248 m, respectively, which are smaller than those of the WMChan-Taylor algorithm. This suggests that incorporating additional error correction into the WMChan-Taylor algorithm enhances positioning stability.

Table 4. Comparison of the positioning parameters in the error-corrected WMChan-Taylor and WMChan-Taylor algorithms.

Algorithm	RMS (m)		RMSE (m)	
	maximum value	average value	X direction	Y direction
WMChan-Taylor	3.340	0.327	0.4401	0.5332
error-corrected WMChan-Taylor	1.496	0.189	0.1729	0.2248

5. Semi-Physical Simulation Analysis

Due to experimental limitations, this paper applies the ultra-wide band (UWB) positioning system to establish an experimental platform and verifies the error-corrected WMChan-Taylor algorithm through semi-physical simulation. UWB is a short-range wireless impulse communication technology with advantages such as low energy consumption, fast transmission, and a simple system. UWB and hydroacoustic positioning technology have similar localization algorithms, both using the corresponding Chan algorithm, Taylor series expansion algorithm, and Chan-Taylor algorithm. Therefore, the UWB system can be used to validate the error-corrected WMChan-Taylor algorithm.

Before conducting the experiment, the UWB equipment must be calibrated. The calibration process is detailed in Figure 15. A UWB tag is placed on a four-wheeled trolley, which is controlled to move within the area surrounded by UWB stations. A right-angle coordinate system is constructed with station 0 as the coordinate origin in meters. The direction between station 0 and station 1 represents the positive direction of the X axis,

while the direction between station 0 and station 3 represents the positive direction of the Y axis. The calibration process consists of straight-line and turning movements. First, the trolley moves from the marked point (0.80, 2.00) to the point (4.00, 2.00) in a straight line. Then, the trolley moves in a circular motion with the marked point (4.50, 4.00) as the center and a 1.5 m radius. The data obtained during the calibration process is processed using the Kalman filtering algorithm. As a result, the calibrated UWB localization process improved the localization accuracy in the X and Y directions from ±0.15 m and ±0.27 m to ±0.05 m and ±0.12 m, respectively.

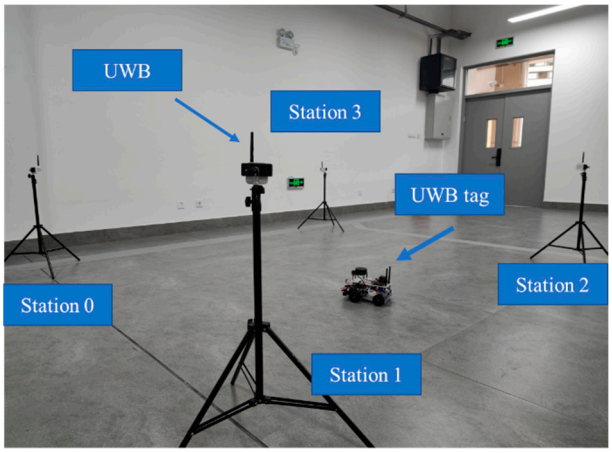

Figure 15. UWB calibration.

The experiment was conducted in a pool measuring 2 m in width and 4 m in length, as depicted in Figure 16. In this setup, a robotic fish equipped with a UWB tag swims on the water surface, as illustrated in Figure 17. As the robotic fish swims, the UWB tag continuously emits electromagnetic wave signals, which undergo multipath propagation due to reflections from the water surface. Additionally, since the experiment takes place indoors, walls also reflect these signals. Consequently, the variation in noise deviation between the receiving stations can be simulated by adjusting the distance L between each station and the wall, as shown in Figure 18.

Figure 16. Experimental environment.

During the experiment, the robotic fish maintained the same tail swing amplitude to ensure a consistent movement speed in the pool. To compare the differences in localization results between the error-corrected WMChan-Taylor algorithm, the WMChan-Taylor algorithm, and the Chan-Taylor algorithm, the value of L was set to 1 m, 0.8 m, 0.6 m, 0.4 m, and 0.2 m. The parameters of each algorithm were kept consistent with the previous simulation conditions.

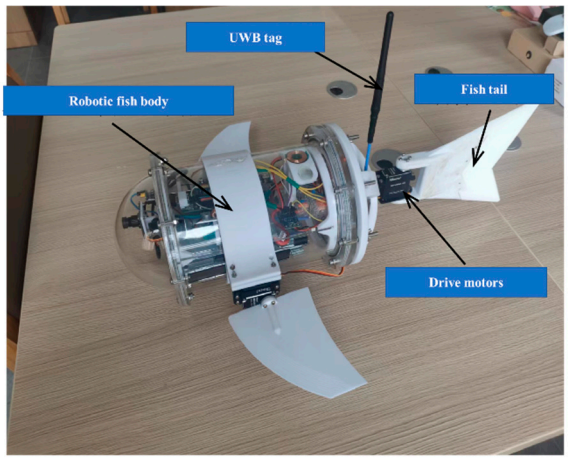

Figure 17. The robotic fish.

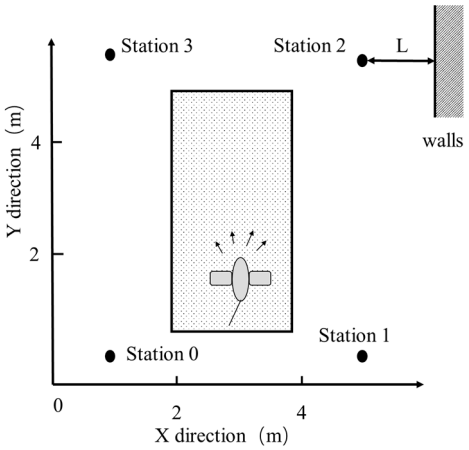

Figure 18. Schematic of the experimental scene.

The experimental results are shown in Figures 19–21. The RMS values exhibit an increasing trend over time because the water surface ripples as the robotic fish swims in the pool, causing the multipath propagation effect of the electromagnetic wave signals to intensify. Since the error-corrected WMChan-Taylor algorithm and the WMChan-Taylor algorithm iteratively measure the noise matrix, their RMS values are lower than the Chan-Taylor algorithm.

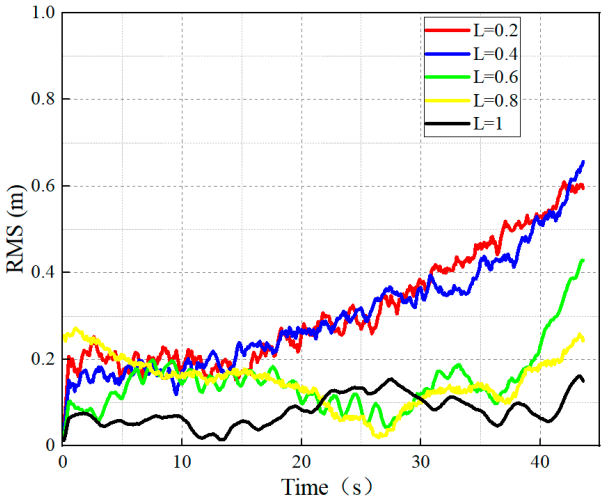

Figure 19. The RMS value variation of the error-corrected WMChan-Taylor algorithm.

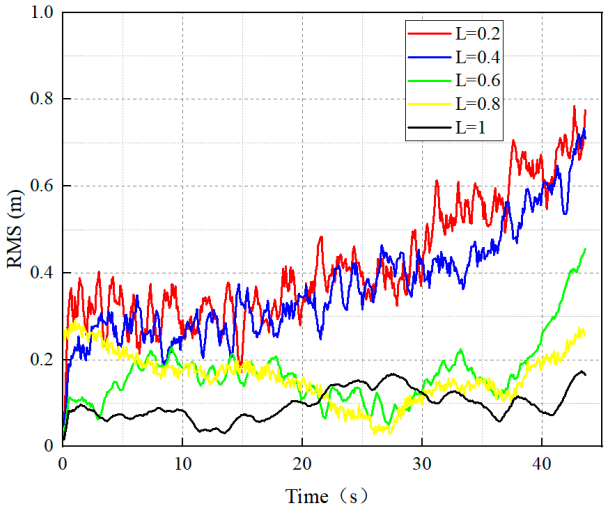

Figure 20. The RMS value variation of the WMChan-Taylor algorithm.

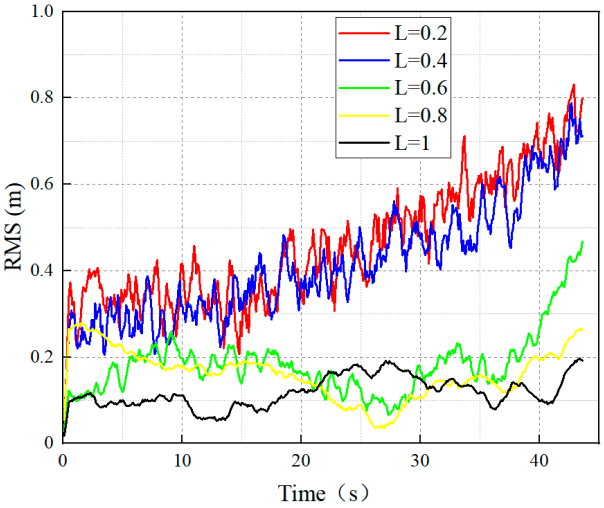

Figure 21. The RMS value variation of the Chan-Taylor algorithm.

When receiving station 2 is at a distance of L = 1 m or 0.8 m from the wall, signal reflections from the wall do not significantly affect station 2 because it is still some distance away. Thus, the RMS values of the error-corrected WMChan-Taylor algorithm, the WMChan-Taylor algorithm, and the Chan-Taylor algorithm are all relatively low, maintaining higher localization accuracy. As L decreases, the effect of wall reflections on station 2 begins to increase. When L = 0.2 m, the WMChan-Taylor algorithm and the Chan-Taylor algorithm have the largest errors, with RMS values of 0.78 m and 0.83 m, respectively. Although the WMChan-Taylor algorithm optimizes the localization results of the Chan-Taylor algorithm, the optimization effect is not obvious at this point. Compared to the WMChan-Taylor algorithm, the maximum RMS value of the error-corrected WMChan-Taylor algorithm at L = 0.2 m is 0.61 m, which is smaller than the RMS value of the WMChan-Taylor algorithm under the same conditions. This indicates that the error-corrected WMChan-Taylor algorithm can isolate station 2, which exhibits larger errors. However, localization accuracy begins to decline as only three receiving stations remain to position the robotic fish following isolation.

Comparing the variation in RMSE values for different values of L, the results are displayed in Figure 22. The error-corrected WMChan-Taylor algorithm demonstrates the smallest change in RMSE values, indicating greater stability. Specifically, when L = 1 m, the noise deviation impact of station 2 is relatively minor. Nonetheless, the RMSE of the

error-corrected WMChan-Taylor algorithm is 0.088 m, which is less than the 0.102 m of the WMChan-Taylor algorithm. This improvement stems from the error-corrected algorithm's use of standardized location-solving combinations and the application of a standard residual weighting to the positional combinations, further correcting the localization error and enhancing result stability.

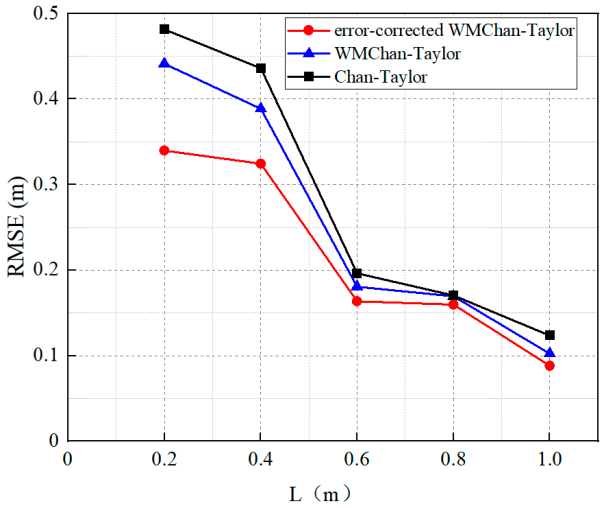

Figure 22. Changes in RMSE values.

Semi-physical simulation experiments demonstrate that the error-corrected WMChan-Taylor algorithm effectively reduces the detrimental effects of NLOS errors and station noise bias on localization results.

6. Conclusions

This paper optimizes the Chan-Taylor algorithm to mitigate the impact of NLOS errors and noise deviations at the receiving stations on the accuracy of AUV hydroacoustic localization solutions. The WMChan-Taylor algorithm is introduced, incorporating dynamic weights into the Chan algorithm to address issues such as long iteration times or dispersion due to large initial value errors from NLOS errors. Simulation results demonstrate that this algorithm effectively uses weights to correct measurement noise variance, optimizes initial values, and enhances localization accuracy. To further address positioning errors caused by varying measurement noise deviations among different receiving stations during underwater positioning, the error-corrected WMChan-Taylor algorithm is proposed. This algorithm introduces a standard residual function to eliminate time delays with large errors at the receiving stations. It applies standard residual weighting to the resultant position solution combinations for further optimization, achieving an optimal combination of positioning solutions. Computer and semi-physical simulation experiments verify that the error-corrected WMChan-Taylor algorithm effectively isolates positioning errors from stations with larger measurement noise variances, significantly enhancing overall positioning accuracy. Moreover, the algorithm improves the stability of the positioning results by implementing weighted processing for the solution combination.

In this paper, the effect of station arrangement on the AUV positioning solution algorithm for hydroacoustic systems was not explored. Future research could integrate the station arrangement with the localization-solving algorithm to enhance the optimization further. Moreover, incorporating intelligent algorithms or Kalman filters may reduce the significant noise bias from the stations during the solution process.

Author Contributions: Conceptualization, H.Y. and X.G.; methodology, H.Y.; validation, H.Y., B.L. and B.X.; data analysis, H.Y. and B.X.; investigation, H.Y.; resources, H.H.; data curation, H.Y. and B.L.; writing—original draft preparation, H.Y.; writing—review and editing, X.G. and H.H.;

visualization, B.L.; funding acquisition, H.H. All authors have read and agreed to the published version of the manuscript.

Funding: This research was funded by Fujian Provincial Department of Science and Technology Unveiled Major Special Project (2023HZ025003); Fujian Provincial Science and Technology Innovation Key Project (2022G02008); Fujian University of Technology High-Level Research Initiation Project (GY-Z23027).

Institutional Review Board Statement: Not applicable.

Informed Consent Statement: Not applicable.

Data Availability Statement: Data are contained within the article.

Conflicts of Interest: The authors declare no conflicts of interests.

References

1. Katzschmann, R.K.; DelPreto, J.; MacCurdy, R.; Rus, D. Exploration of Underwater Life with an Acoustically Controlled Soft Robotic Fish. *Sci. Robot.* **2018**, *3*, eaar3449. [CrossRef] [PubMed]
2. Wright, M.; Xiao, Q.; Dai, S.; Post, M.; Yue, H.; Sarkar, B. Design and Development of Modular Magnetic Bio-Inspired Autonomous Underwater Robot—MMBAUV. *Ocean Eng.* **2023**, *273*, 113968. [CrossRef]
3. Gruber, D.F.; Wood, R.J. Advances and Future Outlooks in Soft Robotics for Minimally Invasive Marine Biology. *Sci. Robot.* **2022**, *7*, eabm6807. [CrossRef] [PubMed]
4. Zhang, B.; Ji, D.; Liu, S.; Zhu, X.; Xu, W. Autonomous Underwater Vehicle Navigation: A Review. *Ocean Eng.* **2023**, *273*, 113861. [CrossRef]
5. Otero, P.; Hernández-Romero, Á.; Luque-Nieto, M.-Á.; Ariza, A. Underwater Positioning System Based on Drifting Buoys and Acoustic Modems. *J. Mar. Sci. Eng.* **2023**, *11*, 682. [CrossRef]
6. Xu, B.; Wang, L.; Li, S.; Zhang, J. A Novel Calibration Method of SINS/DVL Integration Navigation System Based on Quaternion. *IEEE Sens. J.* **2020**, *20*, 9567–9580. [CrossRef]
7. Topini, E.; Topini, A.; Franchi, M.; Bucci, A.; Secciani, N.; Ridolfi, A.; Allotta, B. LSTM-Based Dead Reckoning Navigation for Autonomous Underwater Vehicles. In *Global Oceans 2020: Singapore—U.S. Gulf Coast*; IEEE: New York, NY, USA, 2020.
8. Qin, J.; Li, M.; Li, D.; Zhong, J.; Yang, K. A Survey on Visual Navigation and Positioning for Autonomous UUVs. *Remote Sens.* **2022**, *14*, 3794. [CrossRef]
9. Xu, S.; Wu, L.; Doğançay, K.; Alaee-Kerahroodi, M. A Hybrid Approach to Optimal TOA-Sensor Placement with Fixed Shared Sensors for Simultaneous Multi-Target Localization. *IEEE Trans. Signal Process.* **2022**, *70*, 1197–1212. [CrossRef]
10. Liu, Y.; Subirana, J.S.; Xu, T.; Wang, J.; Yang, W.; Zhang, S.; Shu, J. Ultra-Fast Calculation Method of Incident Angle Based on Underwater Acoustic Round-Trip Positioning. *Ocean Eng.* **2024**, *305*, 117998. [CrossRef]
11. Huang, H.; Zheng, Y.R. Node Localization with AoA Assistance in Multi-Hop Underwater Sensor Networks. *Ad Hoc Netw.* **2018**, *78*, 32–41. [CrossRef]
12. Yamamoto, B.; Wong, A.; Agcanas, P.J.; Jones, K.; Gaspar, D.; Andrade, R.; Trimble, A.Z. Received Signal Strength Indication (RSSI) of 2.4 GHz and 5 GHz Wireless Local Area Network Systems Projected over Land and Sea for Near-Shore Maritime Robot Operations. *J. Mar. Sci. Eng.* **2019**, *7*, 290. [CrossRef]
13. Zheng, Z.; Zhang, H.; Wang, W.-Q.; So, H.C. Source Localization Using TDOA and FDOA Measurements Based on Semidefinite Programming and Reformulation Linearization. *J. Frankl. Inst.* **2019**, *356*, 11817–11838. [CrossRef]
14. Wanchun, L.; Ruibin, C.; Yuning, G.; Caixia, F. Closed Form Algorithm of Double-Satellite TDOA + AOA Localization Based on WGS-84 Model. *Chin. J. Aeronaut.* **2019**, *32*, 2354–2367.
15. Xu, Z.; Li, H.; Yang, K.; Li, P. A Robust Constrained Total Least Squares Algorithm for Three-Dimensional Target Localization with Hybrid TDOA–AOA Measurements. *Circuits Syst. Signal Process.* **2023**, *42*, 3412–3436. [CrossRef]
16. Jiang, L.; Tang, T.; Wu, Z.; Zhao, P. An Iterative Algorithm for the Joint Estimation of Multiple Targets and Observation Stations Using Direction of Arrival and Time Difference of Arrival Measurements despite Station Position Errors. *IET Signal Process.* **2023**, *17*, 12229. [CrossRef]
17. Luo, Y.; Yao, Y.; Xin, M.; Wang, H. Analysis of Static Single-Difference Positioning Errors in Walk-around Underwater Navigation. In Proceedings of the Fourth International Conference on Geology, Mapping, and Remote Sensing (ICGMRS 2023), Wuhan, China, 14–16 April 2023; SPIE: Bellingham, WA, USA, 2024; Volume 12978, pp. 135–141.
18. Hao, K.; Yu, K.; Gong, Z.; Du, X.; Liu, Y.; Zhao, L. An Enhanced AUV-Aided TDoA Localization Algorithm for Underwater Acoustic Sensor Networks. *Mob. Netw. Appl.* **2020**, *25*, 1673–1682. [CrossRef]
19. Chen, H.-H.; Wang, C.-C. Optimal Localization of a Seafloor Transponder in Shallow Water Using Acoustic Ranging and GPS Observations. *Ocean Eng.* **2007**, *34*, 2385–2399. [CrossRef]
20. Bo, X.; Razzaqi, A.A.; Wang, X. Optimal Sensor Formation for 3D Cooperative Localization of AUVs Using Time Difference of Arrival (TDOA) Method. *Sensors* **2018**, *18*, 4442. [CrossRef]
21. Lekkas, A.M.; Candeloro, M.; Schjølberg, I. Outlier Rejection in Underwater Acoustic Position Measurements Based on Prediction Errors. *IFAC-Pap.* **2015**, *48*, 82–87. [CrossRef]

22. Dehghani, H.L.; Golmohammadi, S.; Shadi, K. Extract Non-Line-of-Sight State of Base Stations and Error Mitigation Technique for Wireless Localization in Micro-Cell Networks. *Comput. Commun.* **2012**, *35*, 885–893. [CrossRef]
23. Zhou, B.; Zhuang, Y.; Cao, Y. On the Performance Gain of Harnessing Non-Line-of-Sight Propagation for Visible Light-Based Positioning. *IEEE Trans. Wirel. Commun.* **2020**, *19*, 4863–4878. [CrossRef]
24. Zhang, L.; Zhang, T.; Shin, H.-S. An Efficient Constrained Weighted Least Squares Method With Bias Reduction for TDOA-Based Localization. *IEEE Sens. J.* **2021**, *21*, 10122–10131. [CrossRef]
25. Bai, X.; Dong, L.; Ge, L.; Xu, H.; Zhang, J. Robust Localization of Mobile Robot in Industrial Environments With Non-Line-of-Sight Situation. *IEEE Access* **2020**, *8*, 22537–22545. [CrossRef]
26. Fang, J.; Feng, D.; Li, J. Research on modified Newton and Taylor-series methods in TDOA. *J. Xidian Univ.* **2016**, *43*, 27–33.
27. Zou, Y.; Liu, H.; Wan, Q. An Iterative Method for Moving Target Localization Using TDOA and FDOA Measurement. *IEEE Access* **2018**, *6*, 2746–2754. [CrossRef]
28. Noroozi, A.; Sebt, M.A. Target Localization in Multistatic Passive Radar Using SVD Approach for Eliminating the Nuisance Parameters. *IEEE Trans. Aerosp. Electon. Syst.* **2017**, *53*, 1660–1671. [CrossRef]
29. Yang, H.; Gao, X.; Huang, H.; Li, B.; Xiao, B. An LBL Positioning Algorithm Based on an EMD-ML Hybrid Method. *Eurasip J. Adv. Signal Process.* **2022**, *2022*, 38. [CrossRef]
30. Kulkarni, R.V.; Venayagamoorthy, G.K. Particle Swarm Optimization in Wireless-Sensor Networks: A Brief Survey. *IEEE Trans. Syst. Man Cybern. Part C Appl. Rev.* **2011**, *41*, 262–267. [CrossRef]
31. RejinaParvin, J.; Vasanthanayaki, C. Particle Swarm Optimization-Based Clustering by Preventing Residual Nodes in Wireless Sensor Networks. *IEEE Sens. J.* **2015**, *15*, 4264–4274. [CrossRef]
32. Gharghan, S.K.; Nordin, R.; Ismail, M.; Ali, J.A. Accurate Wireless Sensor Localization Technique Based on Hybrid PSO-ANN Algorithm for Indoor and Outdoor Track Cycling. *IEEE Sens. J.* **2016**, *16*, 529–541. [CrossRef]
33. Chen, H.; Cao, L.; Yue, Y. TDOA/AOA Hybrid Localization Based on Improved Dandelion Optimization Algorithm for Mobile Location Estimation Under NLOS Simulation Environment. *Wirel. Pers. Commun.* **2023**, *131*, 2747–2772. [CrossRef]
34. Yang, H.; Gao, X.; Huang, H.; Li, B.; Jiang, J. A Tightly Integrated Navigation Method of SINS, DVL, and PS Based on RIMM in the Complex Underwater Environment. *Sensors* **2022**, *22*, 9479. [CrossRef]